PSFC/JA-01-30

# Driven reconnection about a magnetic X-line with strong guide component

J.J. Ramos, F. Porcelli and R. Verástegui

November, 2001

Plasma Science and Fusion Center
Massachusetts Institute of Technology
Cambridge MA 02139, U.S.A.

This work was supported by the U.S. Department of Energy under Grant No. DE-FG02-91ER-54109.
Reproduction, translation, publication use and disposal, in whole or in part, by or for the United States government is permitted.

# Driven reconnection about a magnetic X-line with strong guide component

J.J. Ramos, F. Porcelli[†] and R. Verástegui

Plasma Science and Fusion Center, Massachusetts Institute of Technology, Cambridge MA, U.S.A.

[†]Istituto Nazionale Fisica della Materia, Politecnico di Torino, Italy

## Abstract

A two-dimensional, two-fluid model is used to investigate driven magnetic reconnection in collisionless or semi-collisional plasmas. The reconnection is driven by externally induced plasma flows in a background magnetic configuration that has a hyperbolic null in the reconnection plane and a strong component, so called guide component, perpendicular to that plane. Assuming the external drive to be sufficiently weak for a linear approximation to hold, a dynamic evolution of the system is obtained which does not reach a stationary state. The magnetic reconnection proceeds in two phases: an initial one whose characteristic rate is a fraction of the Alfvén frequency, and a later one whose rate is determined by the electron collision frequency.

One of the fundamental goals of magnetic reconnection research is to understand the fast reconnection rates observed to occur in plasmas of low collisionality, both in the space[1] and in the laboratory[2]. A significant part of the theoretical progress made over the past decade comes from a body of work based on a collisionless or semi-collisional, two-fluid description of the plasma[3-14]. In particular, much attention has been devoted to elucidate the effects of the different non-ideal terms in the two-fluid generalized Ohm's law. In the experimental area, facilities such as MRX at the Princeton Plasma Physics Laboratory[15] and VTF at the M.I.T. Plasma Science and Fusion Center[16,17] have been specifically dedicated to study magnetic reconnection in low collisionality regimes. In the VTF device, a toroidal plasma is confined in an externally created magnetic field that has a quadrupole poloidal cusp component and a toroidal or guide component. The relative magnitude of these magnetic field components can be varied to investigate both the weak-guide-field and the strong-guide-field regimes. Reconnection of the poloidal magnetic field is driven by plasma flows towards and away from the poloidal null or X-line, through $\mathbf{E} \times \mathbf{B}$ drifts generated by an externally induced toroidal electric field.

In the present work we use the two-fluid collisionless or semi-collisional formalism, to investigate driven magnetic reconnection in a simplified two-dimensional model that simulates the geometry and conditions of the VTF experiment, in its strong-guide-field regime. The strong guide field guarantees that the plasma is magnetized and makes the fluid description more plausible. We also assume that the ratio $\beta$ between kinetic and magnetic pressures is small, as is the case for VTF. Thus we are concerned with driven reconnection in a background magnetic configuration consisting of a hyperbolic null in the reconnection plane with a strong component perpendicular to it. Such a magnetic configuration has been considered to study driven reconnection as well as resistively damped modes within the framework of single-fluid resistive MHD[18-22], but it has not been investigated within the two-fluid framework appropriate to low collisionality regimes.

In addition to the usual quasineutrality assumption, we choose, for the sake of simplicity, to close the two-fluid MHD system by assuming isotropic stress tensors and constant temperatures. Thus our momentum balance equations read:

$$\sum_{\alpha=e,i} n m_\alpha \Big[ \frac{\partial \mathbf{u}_\alpha}{\partial t} + (\mathbf{u}_\alpha \cdot \nabla)\mathbf{u}_\alpha \Big] \;=\; \mathbf{j} \times \mathbf{B} - \nabla(p_e + p_i), \tag{1}$$

$$\mathbf{E} + \mathbf{u}_i \times \mathbf{B} \;=\; \eta \mathbf{j} + \frac{1}{ne}(\mathbf{j} \times \mathbf{B} - \nabla p_e) - \frac{m_e}{e}\Big[ \frac{\partial \mathbf{u}_e}{\partial t} + (\mathbf{u}_e \cdot \nabla)\mathbf{u}_e \Big], \tag{2}$$

where the index $\alpha = e, i$ labels the electron and (singly charged) ion species, $\mathbf{u}_\alpha$ and $p_\alpha = nT_{\alpha 0}$ stand respectively for their flow velocities and pressures $T_{\alpha 0}$ being their constant temperatures, $m_\alpha$ are the particle masses, $e$ is the magnitude of the electron charge and $n$ is the particle density. Also, $\mathbf{B}$ denotes

the magnetic field, $\mathbf{E}$ the electric field, $\mathbf{j}$ the current density and $\eta$ the collisional resistivity which is assumed to be constant. The electron momentum balance equation (2) has been written in the form of a generalized Ohm's law, showing explicitly on its right hand side the resistive, Hall, electron pressure and electron inertia terms. Our quasineutral, two-fluid MHD system is completed by including the ion continuity equation $\partial n/\partial t + \nabla \cdot (n\mathbf{u}_i) = 0$, Ampere's law $\nabla \times \mathbf{B} = \mathbf{j} = en(\mathbf{u}_i - \mathbf{u}_e)$, and the two homogeneous Maxwell's equations. Then we carry out a two-dimensional reduction by assuming a Cartesian geometry with the hyperbolic magnetic null in the $(x, y)$-plane, the guide component along the $z$-direction and all variables independent of the $z$-coordinate. Thus the magnetic field and the ion flow velocity admit the following representations:

$$\mathbf{B}(x, y, t) \;=\; \mathbf{e}_z \times \nabla\psi(x, y, t) + B_z(x, y, t)\mathbf{e}_z, \tag{3}$$

$$\mathbf{u}_i(x, y, t) \;=\; \mathbf{e}_z \times \nabla\varphi(x, y, t) + \nabla\chi(x, y, t) + u_{iz}(x, y, t)\mathbf{e}_z. \tag{4}$$

We assume an equilibrium of constant density $n_0$, vanishing flow, current and electric field, and a magnetic field with a constant $z$-component and components in the $(x, y)$-plane given by the leading term of a Taylor expansion about a hyperbolic null, i. e. a quadrupole cusp with sources at infinity: $\mathbf{B}_0(x, y) = B'_{c0}(-x\mathbf{e}_x + y\mathbf{e}_y) + B_{z0}\mathbf{e}_z$. The corresponding equilibrium magnetic potential is therefore $\psi_0(x, y) = B'_{c0}xy$. The magnitude of the equilibrium guide field relative to the cusp field is given by the constant with dimensions of length $l_0 \equiv B_{z0}/B'_{c0}$. We can now define the different equilibrium plasma parameters, specifically the ratio between kinetic and magnetic pressures $\beta \equiv 2n_0(T_{e0}+T_{i0})/{B_{z0}}^2$, the electron and ion skin depths ${d_\alpha}^2 \equiv m_\alpha/(e^2 n_0)$, the ion sound gyroradius ${\rho_s}^2 \equiv m_i(T_{e0}+T_{i0})/(e^2{B_{z0}}^2)$ and the Alfvén transit time ${\tau_A}^2 \equiv m_i n_0/{B'_{c0}}^2$. The complete, time dependent solution is written as the sum of equilibrium and perturbation terms: $n(x, y, t) = n_0 + n_1(x, y, t)$, $\psi(x, y, t) = B'_{c0}xy + \psi_1(x, y, t)$ and $B_z(x, y, t) = B_{z0} + B_{z1}(x, y, t)$, so that the current density and the electric field are given by

$$\mathbf{j}(x, y, t) = -\mathbf{e}_z \times \nabla B_{z1}(x, y, t) + \nabla^2\psi_1(x, y, t)\mathbf{e}_z, \tag{5}$$

$$\nabla \times \mathbf{E}(x, y, t) = -\frac{\partial}{\partial t}[\mathbf{e}_z \times \nabla\psi_1(x, y, t) + B_{z1}(x, y, t)\mathbf{e}_z]. \tag{6}$$

The external drive is imposed through the boundary condition that, far away from the separatrices $(x, y \to \pm\infty)$, the $z$-component of the electric field $E_z = \partial\psi_1/\partial t$ approaches the constant $E_\infty$ corresponding to a constant, externally applied electric field $E_\infty\mathbf{e}_z$. We assume this external drive to be sufficiently weak to carry out a linearization of the problem, taking $\psi_1$, $B_{z1}$ (hence $\mathbf{j}$ and $\mathbf{E}$), $n_1$, $\varphi$, $\chi$ and $u_{iz}$ to be linear in $E_\infty$, and neglecting quadratic terms. The linearized two-fluid MHD equations can then be reduced to a coupled system for the perturbed magnetic potential $\psi_1$ and the ion flow potentials $\varphi$ and $\chi$, all other variables being explicitly obtainable from these three.

The next step is to introduce our low-beta, strong-guide-field orderings, specifically $\beta \ll 1$, ${d_i}^2/{l_0}^2 \ll 1$ (hence ${\rho_s}^2/{l_0}^2 \ll \beta$), and $\tau_A \partial/\partial t \sim \rho_s \nabla \sim d_e \nabla \sim 1$. Besides, we neglect the mass ratio $m_e/m_i$ when compared to unity. As a result, the compressional flow potential $\chi$ can also be eliminated and we obtain the reduced system[4,6,10,12]:

$$\frac{\partial}{\partial t}(\nabla^2 \varphi) \;=\; \frac{1}{n_0 m_i}[\psi_0, \nabla^2 \psi_1], \tag{7}$$

$$\frac{\partial}{\partial t}\Big[(1 - {d_e}^2 \nabla^2)\psi_1\Big] \;=\; [\psi_0, (1 - {\rho_s}^2 \nabla^2)\varphi] + \eta \nabla^2 \psi_1, \tag{8}$$

where we have used the notation $[f, g] = \mathbf{e}_z \cdot (\nabla f \times \nabla g)$. The reduced Ohm's law (8) contains the effects of the collisional resistivity, the electron inertia and the Hall term, but no explicit dependence on the ion skin depth $d_i$ (as opposed to the ion sound gyroradius $\rho_s$) remains under the assumed orderings. An additional term involving explicitly the $d_i$ length scale would have had to be kept under the less restrictive assumptions $\beta \ll 1$ and ${\rho_s}^2/{l_0}^2 \ll 1$ but ${d_i}^2/{l_0}^2 \sim 1$. It is illustrative to write down the plane wave dispersion relation that follows from the reduced system (7,8) in the case of a uniform equilibrium magnetic field with Alfvén speed $c_A$:

$$\omega[\omega(1 + {d_e}^2 k^2) - i\eta k^2] = {c_A}^2 {k_\parallel}^2 (1 + {\rho_s}^2 k^2), \tag{9}$$

which is the Alfvén branch of two-fluid MHD in the limit $\beta \ll 1$, ${k_\parallel}^2/k^2 \ll 1$ and ${d_i}^2 {k_\parallel}^2 \ll 1$.

With $\psi_0(x, y) = B'_{c0} xy$, Eqs.(7,8) admit a class of separable solutions of the form $\psi_1(x, y, t) = \psi_1(x, t) + \psi_1(y, t)$ and $\varphi(x, y, t) = \varphi(x, t) - \varphi(y, t)$. Restricting ourselves to these, we can eliminate $\psi_1(x, t)$ and $\varphi(x, t)$ in favor of $j(x, t) \equiv \partial^2 \psi_1(x, t)/\partial x^2$, to obtain the single equation:

$${\tau_A}^2 \frac{\partial^2}{\partial t^2}\Big[\Big(1 - {d_e}^2 \frac{\partial^2}{\partial x^2}\Big) j(x, t)\Big] - {\tau_A}^2 \eta \frac{\partial^3 j(x, t)}{\partial t \partial x^2} \;=\; x^2 \frac{\partial^2 j(x, t)}{\partial x^2} + 3x \frac{\partial j(x, t)}{\partial x} - {\rho_s}^2 \frac{\partial^2}{\partial x^2}\Big[x \frac{\partial}{\partial x}\Big(x \frac{\partial j(x, t)}{\partial x}\Big)\Big]. \tag{10}$$

We solve the above as an initial value problem with vanishing initial current, $j(x, 0) = 0$, and a non-zero initial time derivative $\partial j(x, 0)/\partial t$ which is evaluated according to Eq.(8) from a non-zero initial flow potential $\varphi(x, y, 0)$. The latter is constrained to be consistent with our boundary conditions of a $\mathbf{E} \times \mathbf{B}$ flow driven by the externally applied electric field at far distances:

$$lim_{x,y \to \pm\infty} \varphi(x, y, t) \;=\; \frac{E_\infty}{2B'_{c0}}\, ln \mid \frac{y}{x} \mid, \tag{11}$$

and

$$lim_{x,y \to \pm\infty} E_z(x, y, t) \;=\; E_\infty. \tag{12}$$

These boundary conditions (11,12) are preserved at all times by our evolution equations (7,8), provided they are satisfied at $t = 0$. To this effect, we choose the following initial flow potential:

$$\varphi(x, y, 0) \;=\; \frac{E_\infty}{4B'_{c0}}\, ln\Big(\frac{y^2 + \delta^2}{x^2 + \delta^2}\Big), \tag{13}$$

where $\delta$ is a regularizing parameter with dimensions of length that should be taken greater than or of the order of both $d_e$ and $\rho_s$. Once the time dependent solution $j(x,t)$ has been obtained, Faraday's and Ohm's laws applied at the X-line, $x = y = 0$, yield the reconnection rate:

$$E_z(0,0,t) \;=\; \frac{\partial \psi_1(0,0,t)}{\partial t} \;=\; 2\,\frac{\partial \psi_1(0,t)}{\partial t} \;=\; 2\left[{d_e}^2 \frac{\partial j(0,t)}{\partial t} + \eta j(0,t)\right]. \tag{14}$$

The long time asymptotic behavior of the current density at the X-line can be derived analytically. Introducing the Laplace transformed $J(x,s) = \int_0^\infty dt\; exp(-st)\; j(x,t)$, the Laplace transform version of Eq.(10), including the appropriate initial conditions, can be solved for $x = 0$ and $s \rightarrow 0$ using asymptotic matching techniques. The result is

$$J(0, s \rightarrow 0) \;\simeq\; \frac{E_\infty \tau_A \rho_s}{2\delta^2 ({d_e}^2 s^2 + \eta s)^{1/2}}, \tag{15}$$

so that, inverting the Laplace transform, we get

$$j(0, t \rightarrow \infty) \;\simeq\; \frac{E_\infty \tau_A \rho_s}{2\delta^2 d_e} \qquad for\ \eta = 0, \tag{16}$$

and

$$j(0, t \rightarrow \infty) \;\simeq\; \frac{E_\infty \tau_A \rho_s}{2\delta^2 (\pi \eta t)^{1/2}} \;=\; \frac{E_\infty \tau_A \rho_s}{2\delta^2 d_e (\pi t/\tau_e)^{1/2}} \qquad for\ \eta \neq 0, \tag{17}$$

where we have used the relation $\eta = {d_e}^2/\tau_e$, $\tau_e$ being the electron collision time. The weakly collisional regime of interest in VTF corresponds to $\tau_e \gg \tau_A$.

The complete solution of the above described initial value problem for $j(x,t)$ is obtained numerically. The actual integration of Eq.(10) is carried out in Fourier space, so that spatial boundary conditions are truly satisfied at $x = \pm\infty$ without the recourse to a finite $x - space$ computational domain and the need to introduce the corresponding maximum computational length parameter. We can show that, in Fourier space, the spectral content of the time-dependent current density grows exponentially towards both high and low wavelengths, and that the Fourier transform of Eq.(10) acquires a simple wave-like character when expressed in terms of a logarithmic wavelength variable. Therefore, for any given value of the time, the computational domain in Fourier space can be determined such that the inclusion of the whole range of required spectral wavelengths is guaranteed. We also note that no further parameters are added in the numerical solutions, so that in the collisionless ($\eta = 0$) simulations a truly dissipation-free system is integrated.

Some of our numerical results are shown in Figs.1-4. In Fig.1 we plot the X-line value of the current density $j(0,t)$ versus time, for several values of the dimensionless resistivity parameter $\eta \tau_A/{d_e}^2 = \tau_A/\tau_e$. After an approximately linear rise, the X-line current density approaches a constant in the

collisionless case and decays proportional to $(t/\tau_e)^{-1/2}$ in the resistive cases. Thus the long time behavior of $j(0,t)$ agrees with the analytic prediction (16,17). The cases displayed correspond to the choice $\delta = d_e = \rho_s$, but we have verified the same result for different values of the ratios $\delta/\rho_s$ and $d_e/\rho_s$. The reconnected flux $\psi_{rec}(t) \equiv \psi_1(0,0,t)$ is derived from $j(0,t)$ by integrating Eq.(14), and the corresponding numerical results are plotted in Fig.2. There we observe an initial phase during which the reconnection proceeds linearly in time with a characteristic rate equal to a fraction of the inverse Alfvén time, independent of the resistivity. Subsequently we observe two different behaviors depending on whether or not the resistivity vanishes. In the strictly collisionless case ($\tau_A/\tau_e = 0$), the reconnection practically ends after several Alfvén times and the total amount of reconnected flux is finite. The numerical value of this collisionless reconnected flux is in agreement with the analytic value derived from Eqs.(14,16): $\psi_{rec}(t \to \infty) = E_\infty \tau_A d_e \rho_s/\delta^2$. In the resistive cases, after the initial fast reconnection phase with $\psi_{rec}(t)$ proportional to $t/\tau_A$, for $t > \tau_e$ the system transitions to a slower reconnection phase with $\psi_{rec}(t)$ proportional to $(t/\tau_e)^{1/2}$, reminiscent of the Sweet-Parker[23,24] rate and also in agreement with the analytic prediction from Eqs.(14,17). Figures 3 and 4 illustrate the long time behavior of the current sheet profile. Under the strictly collisionless assumption, the current grows in an approximately linear fashion from its initial seed until its X-line maximum nears saturation. After that, the maximum at the X-line approaches its constant asymptotic value but the spatial profile develops a complex structure with an inner sublayer that shrinks in time without limit, similar to the findings of Ref.4. This shrinking is exponential as shown in Fig.3: for sufficiently long times the current profile is, to a first approximation, given by

$$j(x, t \to \infty) \simeq \frac{E_\infty \tau_A \rho_s}{2\delta^2 d_e} F\Big[\frac{x}{\rho_s} exp\Big(\frac{\rho_s t}{d_e \tau_A}\Big)\Big], \tag{18}$$

where $F$ is a function of a single argument whose form is determined by the early history of the system, and satisfies $F(0) = 1$, $F(\infty) = 0$. The asymptotic formula (18) can also be derived analytically from the long time behavior of Eq.(10) with $\eta = 0$. For non-vanishing resistivity and after its initial linear growth, the X-line maximum of the current density decays proportional to $(t/\tau_e)^{-1/2}$ according to Eq.(17), and the inner width of its spatial profile also decreases without limit. However this shrinking of the current sheet is slower in the resistive cases, where it follows approximately the square root of the time. This is illustrated in Fig.4 for a resistivity-dominated simulation at $\tau_A/\tau_e = 9$: the long time form of the current density profile is now approximated by the empirical fit:

$$j(x, t \to \infty) \simeq \frac{E_\infty \tau_A \rho_s}{2\delta^2 d_e (\pi t/\tau_e)^{1/2}} G\Big(\frac{x t^{1/2} \tau_e^{1/2}}{d_e \tau_A}\Big), \tag{19}$$

where again $G(0) = 1$ and $G(\infty) = 0$.

We have applied our model to a set of parameters representative of strong-guide-field regime experiments in VTF with hydrogen plasma[25]. The corresponding values of the density, tempera-

tures, guide field, cusp field gradient length and applied electric field are respectively $n_0 = 10^{17} m^{-3}$, $T_{i0} \ll T_{e0} = 20eV$, $B_{z0} = 0.0875T$, $l_0 = 7m$ and $E_\infty = 10V/m$. So we have ${\rho_s}^2/{l_0}^2 \simeq 5 \times 10^{-7}$, $\beta \simeq 10^{-4}$ and ${d_i}^2/{l_0}^2 \simeq 10^{-2}$, therefore our low-beta, strong-guide-field conditions are well satisfied. The electron skin depth and the ion sound gyroradius are comparable, $d_e \simeq 3\rho_s$, and the collisionality is fairly low, $\tau_e \simeq 40\tau_A$. Taking $\delta = 2d_e$ in our simulation, we obtain a maximum X-line current density, at the end of its linear rise and before its slow resistive decay sets in, approximately equal to $5 \times 10^3 A/m^2$ which is in agreement with the experimentally measured value. The electrostatic potential in the $(x, y)$-plane far away from the separatrices is $\Phi \simeq B_{z0}\ \varphi \simeq 35\ \ln|y/x|\ V$, also in agreement with the experimental measurement.

In summary, we have developed a model for driven magnetic reconnection in low collisionality plasmas that, despite its mathematical simplicity, yields a number of significant physical results. The assumed low-beta and strong-guide-field orderings imply a generalized Ohm's law where electron inertia, ion sound gyroradius and eventual collisional resistivity define the relevant length scales. Our time dependent solutions show an ever evolving system in which, after an initial linear rise, the inner width of the current layers decreases without limit below the characteristic length scales. The long time rate of this current layer shrinking depends on the collisionality, being exponential in the collisionless case and power-like in the finite resistivity case. The behavior of the maximum current density at the X-line also changes qualitatively when we compare the collisionless case where it approaches a constant at long times, with the resistive case where it decays proportional to $(t/\tau_e)^{-1/2}$. The rate of magnetic reconnection evolves from an initial phase when the reconnected flux grows on an Alfvén-related scale, proportional to $t/\tau_A$, to a later phase when it grows on a resistivity-related scale, proportional to $(t/\tau_e)^{1/2}$; for a strictly collisionless plasma the reconnection ends after the Alfvénic phase and the total amount of reconnected flux is finite. We must point out that our results, obtained with an idealized two-dimensional linear model, are more likely to be physically valid for the initial short times. Clearly, three-dimensional non-linear effects will preclude the sustainement of our ever narrowing current layers. Therefore we might speculate about an intermittent process whereby finite amounts of flux are reconnected in short, Alfvén-scale time intervals, at the end of which secondary instabilities destroy the current sheets once they have become sufficiently narrow, so the cycle can start over again.

We acknowledge many fruitful discussions with A. Fasoli, J. Egedal, P. Catto, J. Hastie, F. Pegoraro and D. Grasso. One of us (R. V.) was supported by a FIENER Grant from Fundación Gómez Pardo, Spain. This work was sponsored by the U.S. Department of Energy under Grant No. DE-FG02-91ER-54109 at the Massachusetts Institute of Technology.

## REFERENCES.


[1] V.M. Vasyliunas, Rev. Geophys. Space Phys. **13**, 303 (1975).

[2] A.W. Edwards et al., Phys. Rev. Lett. **57**, 210 (1986).

[3] A.Y. Aydemir, Phys. Fluids B **4**, 3469 (1992).

[4] M. Ottaviani and F. Porcelli, Phys. Rev. Lett. **71**, 3802 (1993).

[5] T.J. Schep, F. Pegoraro and B.N. Kuvshinov, Phys. Plasmas **1**, 2843 (1994).

[6] R.G. Kleva, J.F. Drake and F. L. Waelbroeck, Phys. Plasmas **2**, 23 (1995).

[7] Z.W. Ma and A. Bhattacharjee, Geophys. Res. Lett. **23**, 1673 (1996).

[8] D. Biskamp, E. Schwarz and J.F. Drake, Phys. Plasmas **4**, 1002 (1997).

[9] D. Biskamp, Phys. Plasmas **4**, 1964 (1997).

[10] E. Cafaro, D. Grasso, F. Pegoraro, F. Porcelli and A. Saluzzi, Phys. Rev. Lett. **80**, 4430 (1998).

[11] M.A. Shay and J.F. Drake, Geophys. Res. Lett. **25**, 3759 (1998).

[12] G. Valori, D. Grasso and H.J. de Blank, Phys. Plasmas **7**, 178 (2000).

[13] M.A. Shay, J.F. Drake, B.N. Rogers and R.E. Denton, J. Geophys. Res. **106**, 3759 (2001).

[14] Z.W. Ma and A. Bhattacharjee, J. Geophys. Res. **106**, 3773 (2001).

[15] M. Yamada, H.T. Ji, S. Hsu, T. Carter, R. Kulsrud, Y. Ono and F. Perkins, Phys. Rev. Lett. **78**, 3117 (1997).

[16] J. Egedal, A. Fasoli, M. Porkolab and D. Tarkowski, Rev. Sci. Instrum. **71**, 3351 (2000).

[17] J. Egedal, A. Fasoli, D. Tarkowski and A. Scarabosio, Phys. Plasmas **8**, 1935 (2001).

[18] I.J.D. Craig and A.N. McClymont, Astrophys. J. **371**, L41 (1991).

[19] A.B. Hassam, Astrophys. J. **399**, 159 (1992).

[20] S.V. Bulanov, S.G. Shasharina and F. Pegoraro, Plasma Phys. Control. Fusion **34**, 33 (1992).

[21] L. Ofman, P.J. Morrison and R.S. Steinolfson, Astrophys. J. **417**, 748 (1993).

[22] M. De Benedetti and F. Pegoraro, Plasma Phys. Control. Fusion **37**, 103 (1995).

[23] P.A. Sweet, in IAU Symp. 6, Electromagnetic Phenomena in Cosmical Physics, B. Lehnert ed. (Cambridge University Press, 1958) p.123.

[24] E.N. Parker, Astrophys. J. **138**, 552 (1963).

[25] J. Egedal and A. Fasoli, private communication.

## FIGURE CAPTIONS.

Fig.1. Time dependence of the normalized X-line current density, for different values of the resistivity parameter $\tau_A/\tau_e = \eta\tau_A/{d_e}^2$. The dashed lines indicate the long time asymptotic behavior in the resistive cases.

Fig.2. Time dependence of the normalized reconnected flux for different values of the resistivity.

Fig.3. Normalized current density profiles in a collisionless simulation at four different times, showing their asymptotic scaling invariance.

Fig.4. Normalized current density profiles in a resistive simulation at four different times, showing their approximate scaling invariance.

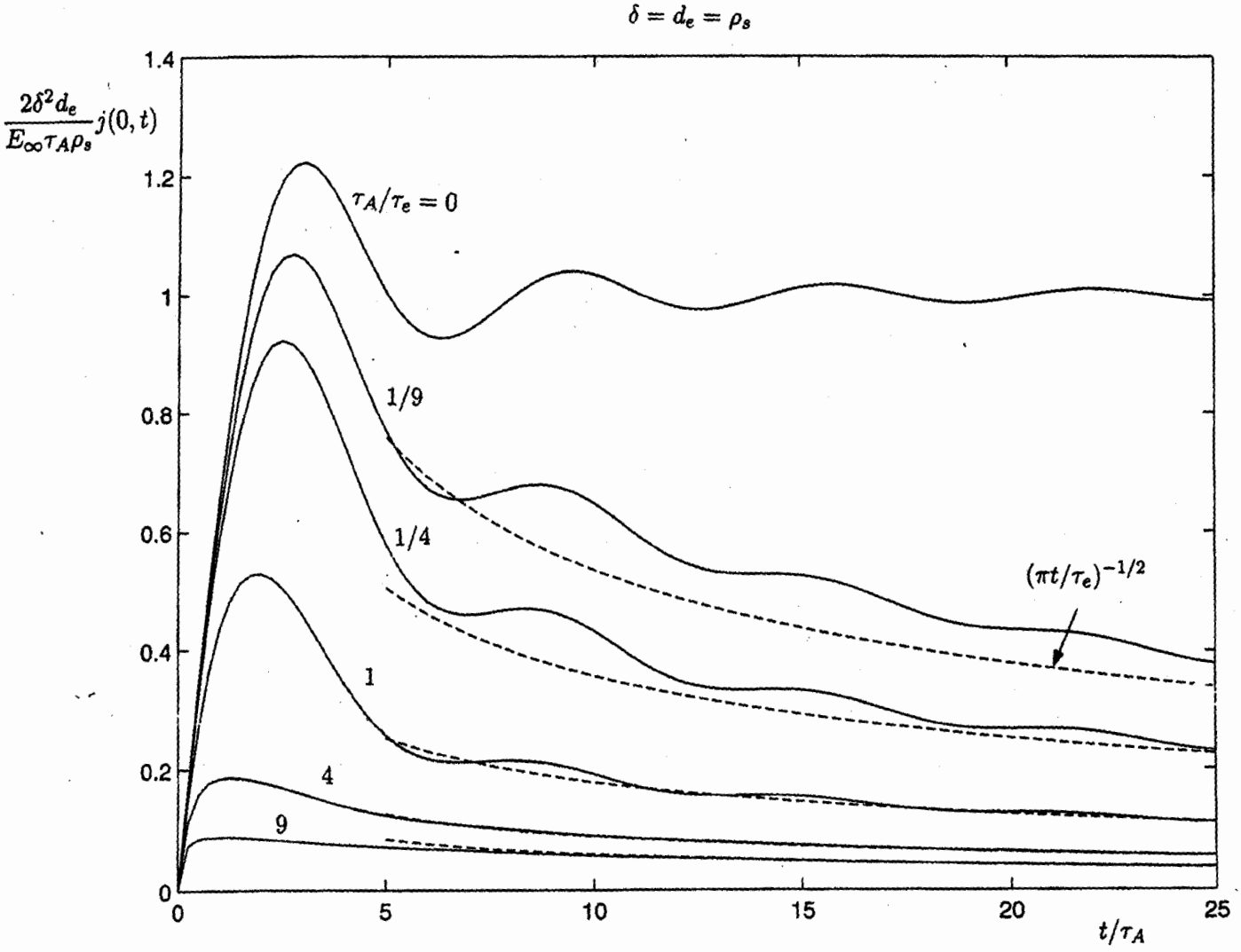
$\delta = d_e = \rho_s$
$\frac{2\delta^2 d_e}{E_\infty \tau_A \rho_s} j(0,t)$
1.4
1.2
1
0.8
0.6
0.4
0.2
0
0
5
10
15
20
25
$t/\tau_A$
$\tau_A/\tau_e = 0$
1/9
1/4
1
4
9
$(\pi t/\tau_e)^{-1/2}$

Figure 1.

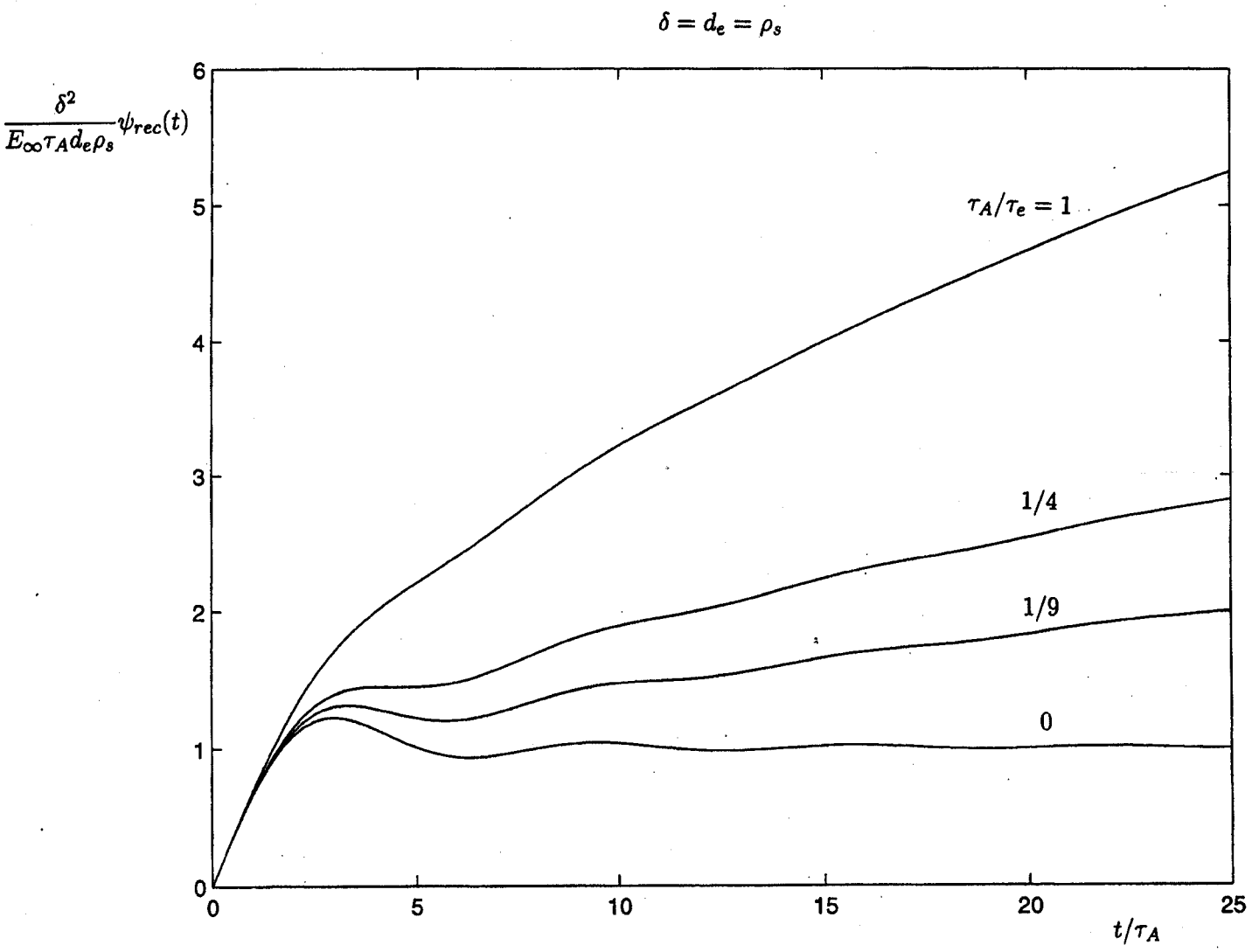
$\delta = d_e = \rho_s$
$\frac{\delta^2}{E_\infty \tau_A d_e \rho_s} \psi_{rec}(t)$
$\tau_A/\tau_e = 1$
1/4
1/9
0
$t/\tau_A$
0
1
2
3
4
5
6
0
5
10
15
20
25

Figure 2.

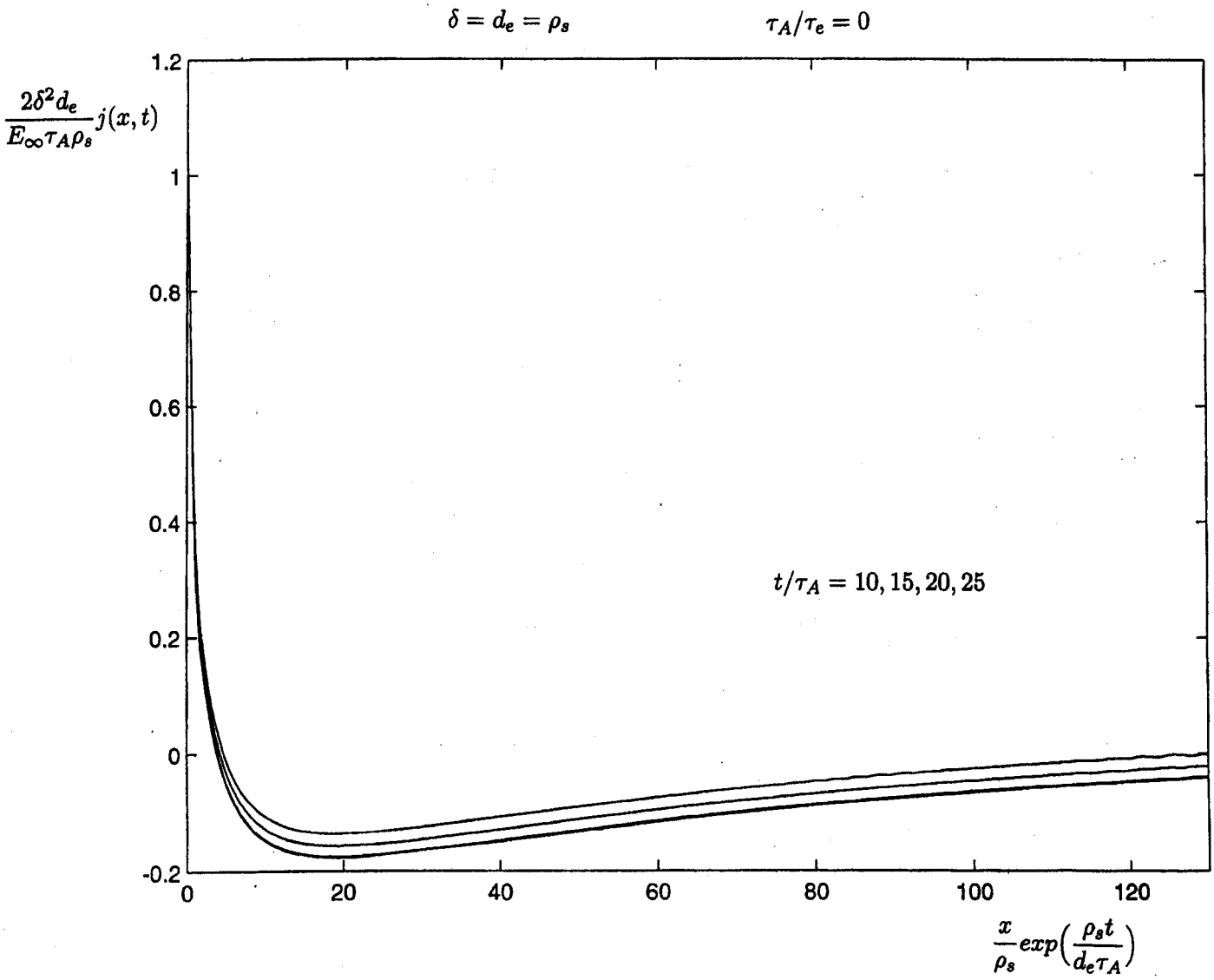
$\delta = d_e = \rho_s$
$\tau_A/\tau_e = 0$
$\frac{2\delta^2 d_e}{E_\infty \tau_A \rho_s} j(x,t)$
1.2
1
0.8
0.6
0.4
0.2
0
-0.2
0
20
40
60
80
100
120
$t/\tau_A = 10, 15, 20, 25$
$\frac{x}{\rho_s} exp\left(\frac{\rho_s t}{d_e \tau_A}\right)$

Figure 3.

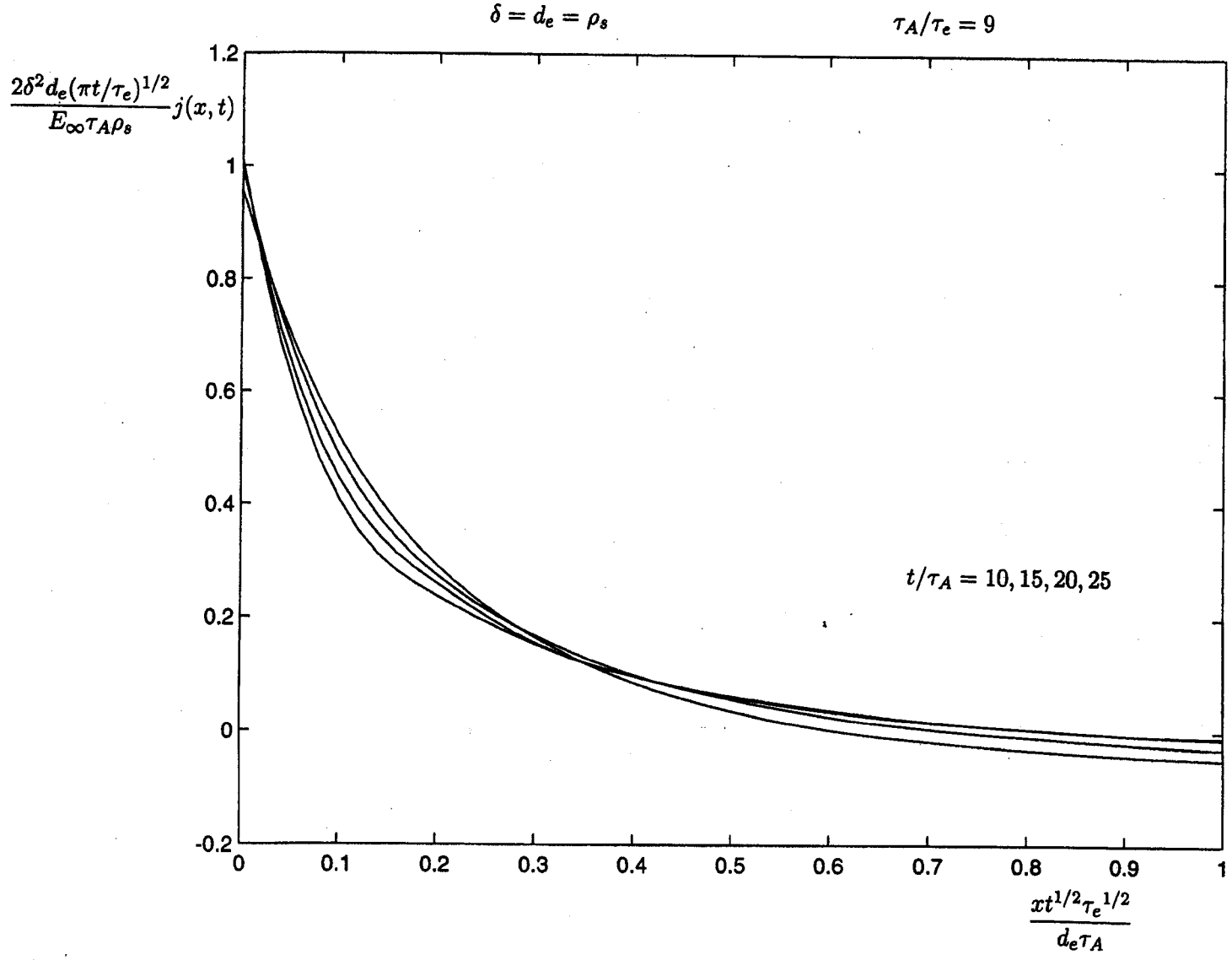
$\delta = d_e = \rho_s$
$\tau_A/\tau_e = 9$
$\frac{2\delta^2 d_e(\pi t/\tau_e)^{1/2}}{E_\infty \tau_A \rho_s} j(x,t)$
1.2
1
0.8
0.6
0.4
0.2
0
-0.2
0
0.1
0.2
0.3
0.4
0.5
0.6
0.7
0.8
0.9
1
$t/\tau_A = 10, 15, 20, 25$
$\frac{x t^{1/2} \tau_e^{1/2}}{d_e \tau_A}$

Figure 4.